

Supplementary Material Cover Sheet

Mobility of biochar-derived dissolved organic matters and their effects on sulfamerazine transport through saturated soil porous media

Mengya Liu ^{1,2}, Xiaochen Liu ³, Yalu Hu ¹, Qiang Zhang ⁴, Usman Farooq ²,
Zhichong Qi ^{2,*}, Laotao Lu ^{5,**}

¹ MOE Key Laboratory of Groundwater Circulation and Environmental Evolution,
China University of Geosciences (Beijing), Beijing 100083, P. R. China

² Henan Joint International Research Laboratory of Environmental Pollution Control
Materials, College of Chemistry and Molecular Sciences, Henan University, Kaifeng
475004, P. R. China

³ Hydrogeology and Engineering Geology Institute of Hubei Geological Bureau, Jinzhou,
434020, P.R. China

⁴ Ecology institute of the Shandong academy of sciences, Qilu University of Technology
(Shandong Academy of Sciences), Jinan 250353, P. R. China

⁵ College of Hydraulic Science and Engineering, Yangzhou University, Yangzhou,
225009, P. R. China

Manuscript prepared for *Environmental Science: Processes & Impacts*

*Corresponding author: Zhichong Qi (qizhichong1984@163.com);

**Corresponding author: Taotao Lu (Taotao.Lu@yzu.edu.cn).

Number of pages: 36

Number of tables: 6

Number of figures: 13

S1. Particle size distribution (PSD) of soil

In this work, the particle size distribution (PSD) of soil grains was measured by the sieve-pipette method (SPM). The SPM is based on the Stokes' Law.^{S1} Soil was dispersed using an ultrasonic vibrator (ca. 20 g soil and ca. 60 mL water in a beaker; sonicated for 2 min). The soil fraction was collected by passing the soil-water suspension through a 53- μm sieve. A 50 mL sample of suspension ($< 53 \mu\text{m}$) was collected to measure silt plus clay. The suspension was allowed to settle for 8 h in a temperature-controlled room (20 °C), and a sample was collected with a 50-mL pipette from a depth of 10 cm for determination of clay.^{S1} Clay ($< 2 \mu\text{m}$), silt (2–53 μm), and sand (53–2 000 μm) contents were calculated as the percentage (%) of recovered sample mass based on the USDA soil texture classification system.

S2. Determination of the CEC of soil

The cation exchange capacity (CEC) of soil was measured by the following the previously reported method. ^{S2} In brief, 500 mL of CaCl₂ (1eq/L) are injected from bottom to top through a column filled with 10 g of soil. Then, 150 mL of CaCl₂ (0.05 eq/L) is injected followed by 500 mL of KNO₃ (1eq/L). The percolate is collected in 500 mL flask and the total calcium was titrated with EDTA (0.02eq/L) at pH 12 using the Eriochrome Black T as indicator. At the same time, the chloride is titrated with AgNO₃ (0.05eq/L) using the K₂CrO₄ as indicator. The CEC is given by:

$$\text{CEC (meq /100g)} = 2v-5V$$

where v is the volume (mL) of EDTA required for calcium titration and V the volume (mL) of AgNO₃ required for chlorides titration.

S3. Synthetic groundwater

Synthetic groundwater was prepared following a protocol reported elsewhere.^{S3} In brief, 60 mg $\text{MgSO}_4 \cdot 7\text{H}_2\text{O}$, 20 mg KNO_3 , 36 mg NaHCO_3 , 36 mg CaCl_2 , 35 mg $\text{Ca}(\text{NO}_3)_2$, and 25 mg $\text{CaSO}_4 \cdot 2\text{H}_2\text{O}$ were added to 1 L of deionized water. The distribution and concentration of different ions in synthetic groundwater are reported in Table S2.

S4. Calculation of UV–vis indexes

Absorbance was measured using a TU-1810PC UV–vis spectrophotometer (Beijing Purkinje General Instrument Co., Beijing, China) within a spectrum of 250–700 nm, at 1-nm increments, using a 1-cm quartz cuvette. Samples were allowed to come to room temperature before measurements were taken. The absorption coefficient a (m^{-1}) was calculated for each wavelength (λ) using the equation: ^{S4}

$$a_{\lambda} = 2.303A_{\lambda} / l$$

where A_{λ} is the absorbance and l is the path length of the optical cell in meters (here $l = 0.01$ m). Measurements for the control were also subtracted after subtracting blank measurements.

SUVA₂₅₄ ($\text{L}/(\text{mg}\cdot\text{C}\cdot\text{m})$) was calculated using the equation:

$$\text{SUVA}_{254} = a_{254} / C_{\text{BDOM}}$$

where a_{254} (m^{-1}) is the absorbance coefficient at 254 nm. C_{BDOM} (mg/L), the BDOM concentration in solution, is 10 mg/L here.

$S_{275-295}$, the spectral slope was determined by fitting an exponential decay model (Sigmaplot Version 11, 2008, Systat Software, Inc.) to the absorption coefficients within the spectra 275–295 nm. ^{S4}

S5. Procedures used to determine relative hydrophobicity of BDOMs

The relative hydrophobicity of **BDOMs** was assessed using a hydrocarbon partitioning test with laboratory-grade *n*-dodecane.^{S5, S6} Samples were prepared by adding 4 mL of BDOMs suspension (10 mg/L) to a test tube containing 1 mL of *n*-dodecane. The test tube was vortexed for 2 min, then left undisturbed for 15 min to allow phase separation. The relative hydrophobicity was assessed as the fraction of biochar colloids partitioned into *n*-dodecane from the aqueous phase.

S6. Determination of the SMZ concentration in the effluent

The SMZ concentration in the effluent in each sample was measured after solvent extraction.^{S7, S8} Specifically, 3 mL of each sample was taken into 10 mL centrifuge tubes with 0.5 mL 0.25 M NaH₂PO₄ and 0.5 mL acetonitrile. Then, the vials were shaken at 25 °C in the dark for 2 h. Afterward, the samples were sonicated for 45 min to free the antibiotics associated with BDOM, immediately filtered through 0.1 µm pore size polytetrafluoroethylene membrane for analysis. The concentration of SMZ was analyzed directly by using a Waters high performance liquid chromatography system (HPLC, e2695, Waters Alliance) equipped with a symmetry reversed-phase C18 column (4.6 × 150 mm) using a UV/visible detector at a wavelength of 265 nm.

S7. Effects of BDOMs on the adsorption of SMZ to soil grains

To better understand the effects of BDOMs on the binding affinities of soil grains for SMZ at different solution chemistry conditions, sorption experiments were conducted to examine the adsorption of SMZ to soil grains with or without BDOMs. For batch experiments, 5 g soil was mixed with 20 mL solution containing 1 mg/L of SMZ and 10 mg/L BDOMs in certain electrolyte solution in glass vials. The solution pH was adjusted by the addition of 0.1 M NaOH or 0.1 M HCl. The mixtures were continuously agitated for a period of 12 h on a rotary shaker maintained at a temperature of 25°C. This duration of agitation was equivalent to the duration of the mobility experiment. Following this, the samples were centrifuged at a rate of 5000 rpm for a period of 20 minutes. The concentrations of SMZ in the supernates (i.e., C_e (mg/L)) were identified by using HPLC after solvent extraction (see Section S5 of Supplementary Material). The mass of SMZ adsorbed to soil grains (i.e., q , in mg/kg) was determined using the mass balance method. The calculation of the distribution coefficients (K_d) of SMZ between soil grains and the aqueous phase was performed using the equation $K_d = q/C_e$. The K_d values were expressed in terms of L/kg.

S8. Procedures used to determine the concentrations of BDOM-adsorbed SMZ in the influents

A negligible depletion solid-phase micro extraction approach was used to determine the concentrations of dissolved and BDOM-adsorbed phenanthrene or 1-naphthol in the influents without having to separate the aqueous solution from the BDOM. ^{S9} Briefly, after an influent was prepared, aliquots of the influent were transferred to amber glass vials, and a piece of glass optical fiber was added to each of the vials (the fibers used were coated with polyacrylate (thickness 35 μm ; volume 15.4 $\mu\text{L}/\text{m}$), and were purchased from Polymicro Technologies (Phoenix, AZ); prior to being used, the fibers were cut to the 5-cm length, and cleaned three times with 50/50 methanol/water (v/v) by shaking, then washed with ultrapure water to remove all the solvent, and stored in water). Next, the vials were tumbled end-over-end for 12 h. This duration of agitation was equivalent to the duration of the mobility experiment. Finally, the fibers were taken out, wiped with wet tissues, and extracted with methanol to analyze the mass of SMZ on the fibers. The concentrations of freely dissolved SMZ were calculated based on the concentrations on the fibers and the sorption isotherms of the compounds to the fiber. The concentrations of SMZ on BDOM (i.e., q , in mg/g) were calculated based on a mass balance approach.

S9. Transport model

The program CXTFIT 2.0 was used to simulate the one-dimensional transport of SMZ.^{S10} The transport of SMZ in a steady-state can be described by the one dimensionless advection-dispersion-reaction (ADR) equation as follow: ^{S11}

$$R \frac{\partial C}{\partial t} = D \frac{\partial^2 C}{\partial x^2} - v \frac{\partial C}{\partial x} \quad (1)$$

where D (m²/d) is the hydrodynamic dispersion coefficient for SMZ, C (mg/L) is the contaminant concentration in the solution-phase, x (m) is distance, v (m/d) is the velocity of pore water, t (d) is time, and R (-) is the retardation factor, which is defined as:

$$R = 1 + \frac{\rho_b}{\theta} \cdot K_d \quad (2)$$

where ρ_b (g/cm³) and θ (-) are the bulk density and porosity of the soil column correspondingly, K_d (L/kg) is the partition coefficient equilibrium models.

However, solutes may not be able to reach equilibrium within the flow domain. In this study, the two-site nonequilibrium transport model was used Nkedi-Kizza et al.^{S12} This model is based on the assumption that there are two different types of sorption sites, an equilibrium site and a kinetic site.^{S13} Moreover, the model assumes that the instantaneous equilibrium site already reaches an equilibrium whereas the kinetic site does not. ^{S13} The concentration of a solute in each site at equilibrium is given as follows:

$$\beta R \frac{\partial C_1}{\partial T} = \frac{1}{P} \frac{\partial^2 C_1}{\partial X^2} - \frac{\partial C_1}{\partial X} - \omega(C_1 - C_2) \quad (3)$$

$$(1 - \beta)R \frac{\partial C_2}{\partial T} = \omega(C_1 - C_2) \quad (4)$$

where parameters without dimensions are as follows:

$$X = \frac{x}{L} \quad (5)$$

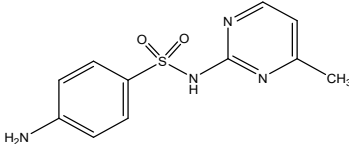
$$P = \frac{vL}{D} \quad (6)$$

$$\beta = \frac{\theta + f\rho_b K_d}{\theta + \rho_b K_d} \quad (7)$$

$$\omega = \frac{\alpha(1-\beta)RL}{v} \quad (8)$$

where C_1 and C_2 (mg/L) are the solute concentrations in sorption sites 1 and 2 respectively, β represents the fraction of the instantaneous equilibrium adsorption sites in all the adsorption sites;^{S14} $f(-)$ is the fraction of Type 1 sites; α (1/d) is the first-order rate coefficient for kinetics at Type 2 sites; and ω is the Damkohler number, indicating the ratio of the reaction rate to the transport rate.^{S15} By fitting conservative tracer (Br⁻) curves using the 2.1 code of CXTFIT, the value for dispersion coefficient (D) was evaluated (Fig. S2).^{S5} We supposed that the SMZ's D value is the same as that in the column for the bromide (0.375 m²/d).^{S16} By matching the breakthrough curve of the SMZ, the value of R , β and ω was achieved. The K_d , f and α values were determined with equations 2, 7, 8.

Table S1. Selected properties of sulfamerazine.

Antibiotics	abbreviation	Molecular formula	Chemical structure	Molecular weight (g/mol)	Log K_{ow} ^a	pK_a ^b
Sulfamerazine	SMZ	$C_{11}H_{12}N_4O_2$ S		264.3	0.44	$pK_{a1}=2.30$ $pK_{a2}=6.80$

^a Derived from Ahmed et al. ^{S17}

^b Dissociation coefficients, derived from Teixido et al.. ^{S18}

Table S2. Recipe of artificial groundwater.

ions	concentration (mM)
HCO ₃ ⁻	0.43
SO ₄ ²⁻	0.39
NO ₃ ⁻	0.62
Cl ⁻	0.64
Ca ²⁺	0.68
Mg ²⁺	0.24
Na ⁺	0.43
K ⁺	0.20

Table S3. Assignments of FTIR spectrum. ^{S19, S20}

Wavenumber	Assignments
3311~3494 cm ⁻¹	H-bonded hydroxyl groups or amino groups
2854~2931 cm ⁻¹ , 1370~1458 cm ⁻¹	aliphatic C-H
1500~1620 cm ⁻¹	aromatic C=C
1700~1750 cm ⁻¹	C=O of carboxyl, aldehyde, ketone, and ester groups
1103~1205 cm ⁻¹	C-O or C-N
745~881 cm ⁻¹	aromatic C-H or C=C-H

Table S4. Experimental setups and breakthrough results of column experiments.

Column No.	Influent properties					Adsorbed mass of SMZ to BDOMs (q , mg/g) ^c	Effluent properties ^d		The retained mass of BDOM in column ^e (%)	The retained mass of SMZ in column ^e (%)
	BDOM ^a	SMZ conc. ^l (mg/L)	Background solution	pH	Flow rate (cm/min)		C/C_0 BDOM(%)	C/C_0 SMZ (%)		
1	BDOM_300	/	10 mM NaCl	7.0	0.29	/	45.6 ± 0.7	/	70.7 ± 0.5	/
2	BDOM_450	/	10 mM NaCl	7.0	0.29	/	33.6 ± 0.3	/	78.2 ± 0.3	/
3	BDOM_600	/	10 mM NaCl	7.0	0.29	/	25.9 ± 0.7	/	83.7 ± 0.2	/
4	/	1	10 mM NaCl	7.0	0.29	/	/	77.7 ± 1.5	/	55.4 ± 0.7
5	BDOM_300	1	10 mM NaCl	7.0	0.29	13.4 ± 1.4	54.1 ± 1.1	81.5 ± 1.1	68.5 ± 0.5	48.7 ± 2.2
6	BDOM_450	1	10 mM NaCl	7.0	0.29	22.5 ± 1.5	39.7 ± 0.1	83.8 ± 0.4	73.0 ± 0.3	36.8 ± 0.1
7	BDOM_600	1	10 mM NaCl	7.0	0.29	32.6 ± 2.8	29.7 ± 0.3	91.0 ± 1.7	77.9 ± 0.8	32.2 ± 0.6
8	BDOM_450	/	10 mM NaCl	5.0	0.29	/	29.7 ± 0.6	/	82.2 ± 0.3	/
9	/	1	10 mM NaCl	5.0	0.29	/	/	73.6 ± 2.6	/	62.2 ± 1.2
10	BDOM_450	1	10 mM NaCl	5.0	0.29	27.6 ± 1.9	35.5 ± 0.1	82.3 ± 0.3	75.2 ± 0.4	39.6 ± 0.7
11	BDOM_450	/	10 mM NaCl	9.0	0.29	/	39.5 ± 0.5	/	75.3 ± 0.4	/
12	/	1	10 mM NaCl	9.0	0.29	/	/	92.4 ± 1.6	/	45.5 ± 0.3
13	BDOM_450	1	10 mM NaCl	9.0	0.29	16.3 ± 2.1	43.1 ± 0.6	97.0 ± 0.4	70.9 ± 0.5	36.6 ± 0.7
14	BDOM_450	/	0.1 mM CaCl ₂	5.0	0.29	/	34.5 ± 0.3	/	76.4 ± 0.1	/
15	/	1	0.1 mM CaCl ₂	5.0	0.29	/	/	63.2 ± 0.3	/	56.7 ± 0.5
16	BDOM_450	1	0.1 mM CaCl ₂	5.0	0.29	35.7 ± 2.6	45.9 ± 0.6	74.5 ± 1.0	67.2 ± 0.4	45.1 ± 0.7
17	BDOM_450	/	0.1 mM CuCl ₂	5.0	0.29	/	14.7 ± 0.5	/	92.3 ± 0.2	/
18	/	1	0.1 mM CuCl ₂	5.0	0.29	/	/	30.2 ± 2.2	/	76.3 ± 1.2
19	BDOM_450	1	0.1 mM CuCl ₂	5.0	0.29	47.6 ± 1.0	25.6 ± 0.4	46.8 ± 0.6	84.0 ± 0.2	67.9 ± 0.8
20	BDOM_450	/	10 mM NaCl	7.0	0.18	/	29.0 ± 0.2	/	81.1 ± 0.1	/
21	/	1	10 mM NaCl	7.0	0.18	/	/	66.3 ± 1.2	/	58.2 ± 0.9
22	BDOM_450	1	10 mM NaCl	7.0	0.18	22.5 ± 1.5	34.2 ± 0.1	78.3 ± 0.1	74.6 ± 0.2	37.5 ± 0.3
23	BDOM_450	/	10 mM NaCl	7.0	0.51	/	40.0 ± 0.6	/	73.5 ± 0.3	/
24	/	1	10 mM NaCl	7.0	0.51	/	/	90.3 ± 0.3	/	42.1 ± 0.1
25	BDOM_450	1	10 mM NaCl	7.0	0.51	22.5 ± 1.5	44.5 ± 0.1	96.1 ± 0.2	68.3 ± 0.1	30.9 ± 0.3
26	BDOM_450	/	artificial groundwater	7.0	0.29	/	36.9 ± 0.3	/	75.2 ± 0.2	/
27	/	1	artificial groundwater	7.0	0.29	/	/	57.3 ± 0.7	/	51.2 ± 0.2
28	BDOM_450	1	artificial groundwater	7.0	0.29	37.9 ± 0.8	45.2 ± 0.2	61.2 ± 0.7	66.1 ± 0.5	42.8 ± 0.5

^a BDOM represents corn straw biochar-derived dissolved organic matter; the suffixes range from 300,450, and 600 represent the pyrolysis temperature.

^b conc. represents concentration.

^c The adsorbed mass of SMZ to BDOMs in the influent. The data were obtained based on the sorption experiments.

^d Average value of last three data points of respective breakthrough curve. C/C_0 represents the ratio of BDOM/SMZ concentration in the effluent to the BDOM/SMZ concentration in the influent.

^e Mass retained in column = 100 – effluent mass.

Table S5. ζ -potential values (mV) of soil under various conditions.

No.	Background solution	pH	ζ -potentials (mV)
1	10 mM NaCl	5.0	-20.2 \pm 1.5
2	10 mM NaCl + BDOM_450	5.0	-23.1 \pm 0.9
3	10 mM NaCl	7.0	-25.7 \pm 0.7
4	10 mM NaCl + BDOM_300	7.0	-28.7 \pm 1.1
5	10 mM NaCl + BDOM_450	7.0	-29.3 \pm 0.3
6	10 mM NaCl + BDOM_600	7.0	-30.5 \pm 0.8
7	10 mM NaCl	9.0	-31.3 \pm 0.5
8	10 mM NaCl + BDOM_450	9.0	-34.6 \pm 1.0
9	0.1 mM CuCl ₂	5.0	-22.5 \pm 0.3
10	0.1 mM CuCl ₂ + BDOM_450	5.0	-25.8 \pm 0.1

Table S6. Fitted parameters of two-site nonequilibrium transport model from breakthrough results of column experiments.

Column No.	BDOM ^a	SMZ conc. ^b (mg/L)	Background solution	pH	Flow rate (cm/min)	Parameters of two-site nonequilibrium transport model						
						<i>R</i> (-)	<i>β</i> (-)	<i>ω</i> (-)	<i>f</i> (-)	<i>α</i> (1/d)	<i>K_d</i> (L/kg)	<i>r</i> ²
4	/	1	10 mM NaCl	7.0	0.29	4.16 ± 0.13	0.421 ± 0.023	0.393 ± 0.017	0.225 ± 0.009	2.41 ± 0.10	1.45 ± 0.07	0.997
5	BDOM_300	1	10 mM NaCl	7.0	0.29	3.95 ± 0.08	0.433 ± 0.017	0.371 ± 0.021	0.240 ± 0.015	2.36 ± 0.13	1.36 ± 0.05	0.998
6	BDOM_450	1	10 mM NaCl	7.0	0.29	3.77 ± 0.12	0.453 ± 0.018	0.316 ± 0.012	0.257 ± 0.011	2.17 ± 0.15	1.25 ± 0.03	0.997
7	BDOM_600	1	10 mM NaCl	7.0	0.29	3.19 ± 0.15	0.497 ± 0.023	0.193 ± 0.005	0.268 ± 0.013	1.71 ± 0.09	1.01 ± 0.01	0.999
9	/	1	10 mM NaCl	5.0	0.29	4.63 ± 0.12	0.327 ± 0.011	0.563 ± 0.021	0.142 ± 0.015	2.56 ± 0.12	1.66 ± 0.05	0.998
10	BDOM_450	1	10 mM NaCl	5.0	0.29	3.54 ± 0.22	0.472 ± 0.025	0.280 ± 0.013	0.272 ± 0.017	2.06 ± 0.07	1.31 ± 0.03	0.990
12	/	1	10 mM NaCl	9.0	0.29	3.11 ± 0.07	0.489 ± 0.018	0.185 ± 0.017	0.250 ± 0.023	1.89 ± 0.10	0.97 ± 0.02	0.993
13	BDOM_450	1	10 mM NaCl	9.0	0.29	2.75 ± 0.03	0.567 ± 0.023	0.139 ± 0.008	0.315 ± 0.012	1.68 ± 0.05	0.77 ± 0.01	0.997
15	/	1	0.1 mM CaCl ₂	5.0	0.29	6.59 ± 0.21	0.288 ± 0.007	0.735 ± 0.035	0.123 ± 0.009	2.89 ± 0.09	2.56 ± 0.04	0.993
16	BDOM_450	1	0.1 mM CaCl ₂	5.0	0.29	5.23 ± 0.09	0.357 ± 0.007	0.619 ± 0.13	0.205 ± 0.005	2.62 ± 0.11	1.93 ± 0.05	0.998
18	/	1	0.1 mM CuCl ₂	5.0	0.29	9.20 ± 0.17	0.149 ± 0.012	0.893 ± 0.035	0.046 ± 0.009	3.62 ± 0.06	3.74 ± 0.03	0.987
19	BDOM_450	1	0.1 mM CuCl ₂	5.0	0.29	7.19 ± 0.11	0.213 ± 0.010	0.713 ± 0.022	0.118 ± 0.010	3.15 ± 0.21	2.83 ± 0.10	0.989
21	/	1	10 mM NaCl	7.0	0.18	4.11 ± 0.08	0.521 ± 0.015	0.472 ± 0.013	0.198 ± 0.011	2.32 ± 0.07	1.43 ± 0.09	0.996
22	BDOM_450	1	10 mM NaCl	7.0	0.18	3.26 ± 0.01	0.495 ± 0.009	0.335 ± 0.010	0.282 ± 0.013	1.95 ± 0.11	1.03 ± 0.01	0.994
24	/	1	10 mM NaCl	7.0	0.51	3.02 ± 0.13	0.502 ± 0.026	0.173 ± 0.013	0.265 ± 0.008	1.53 ± 0.19	0.92 ± 0.03	0.995
25	BDOM_450	1	10 mM NaCl	7.0	0.51	2.53 ± 0.09	0.595 ± 0.016	0.123 ± 0.010	0.330 ± 0.015	1.60 ± 0.07	0.68 ± 0.01	0.996
27	/	1	artificial groundwater	7.0	0.29	5.82 ± 0.21	0.324 ± 0.031	0.723 ± 0.20	0.183 ± 0.016	2.75 ± 0.19	2.20 ± 0.09	0.991
28	BDOM_450	1	artificial groundwater	7.0	0.29	5.17 ± 0.16	0.416 ± 0.023	0.651 ± 0.17	0.256 ± 0.022	2.32 ± 0.13	1.91 ± 0.15	0.989

^a BDOM represents corn straw biochar-derived dissolved organic matter; the suffixes range from 300,450, and 600 represent the pyrolysis temperature.

^b conc. represents concentration.

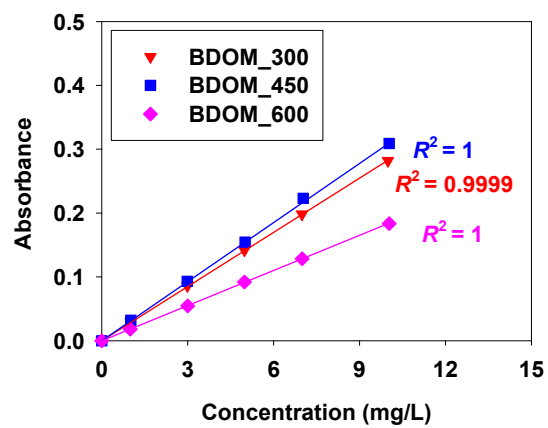


Fig. S1. Calibration curve as absorbance vs. concentration of BDOM (absorbance at the wavelength of 380 nm).

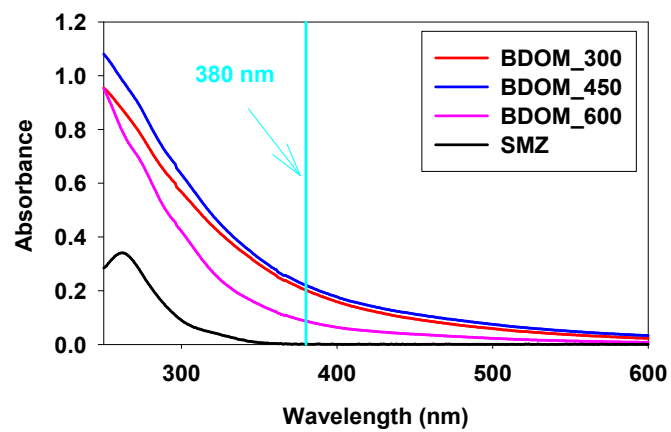


Fig. S2. UV-Vis spectra of BDOM (10 mg/L) and SMZ (1 mg/L) dispersed in DI water.

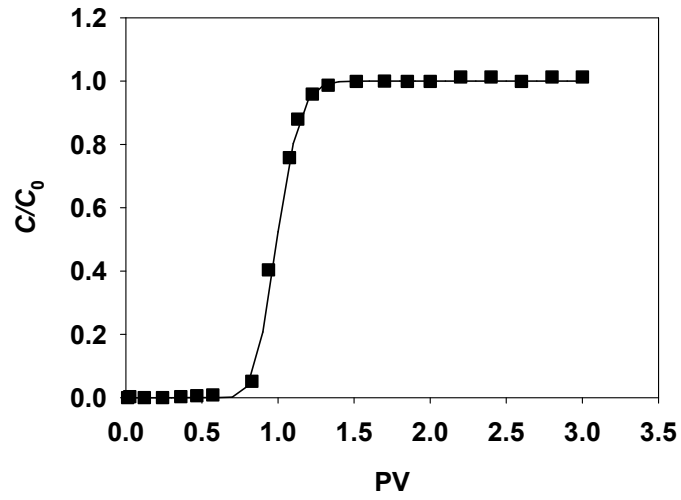


Fig. S3. The representative breakthrough curve of conservative tracer (Br⁻). The line was plotted by fitting the breakthrough data with the one-dimensional steady-state advection-dispersion equation.

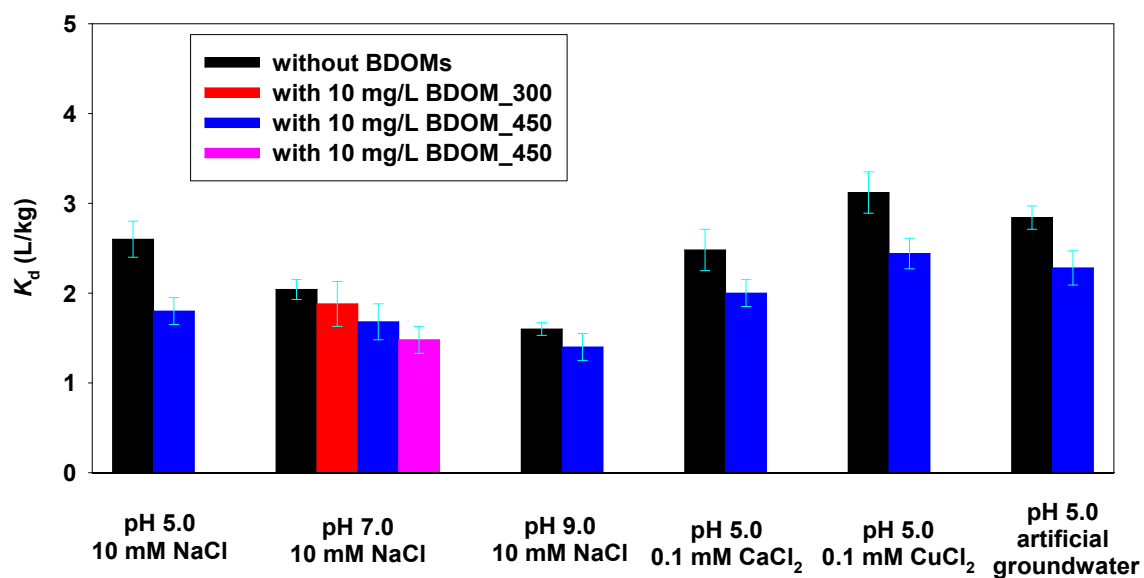


Fig. S4. Adsorption coefficients (K_d) of SMZ to soil grains in the absence or presence of BDOMs. Error bars indicate standard deviation of three replicates.

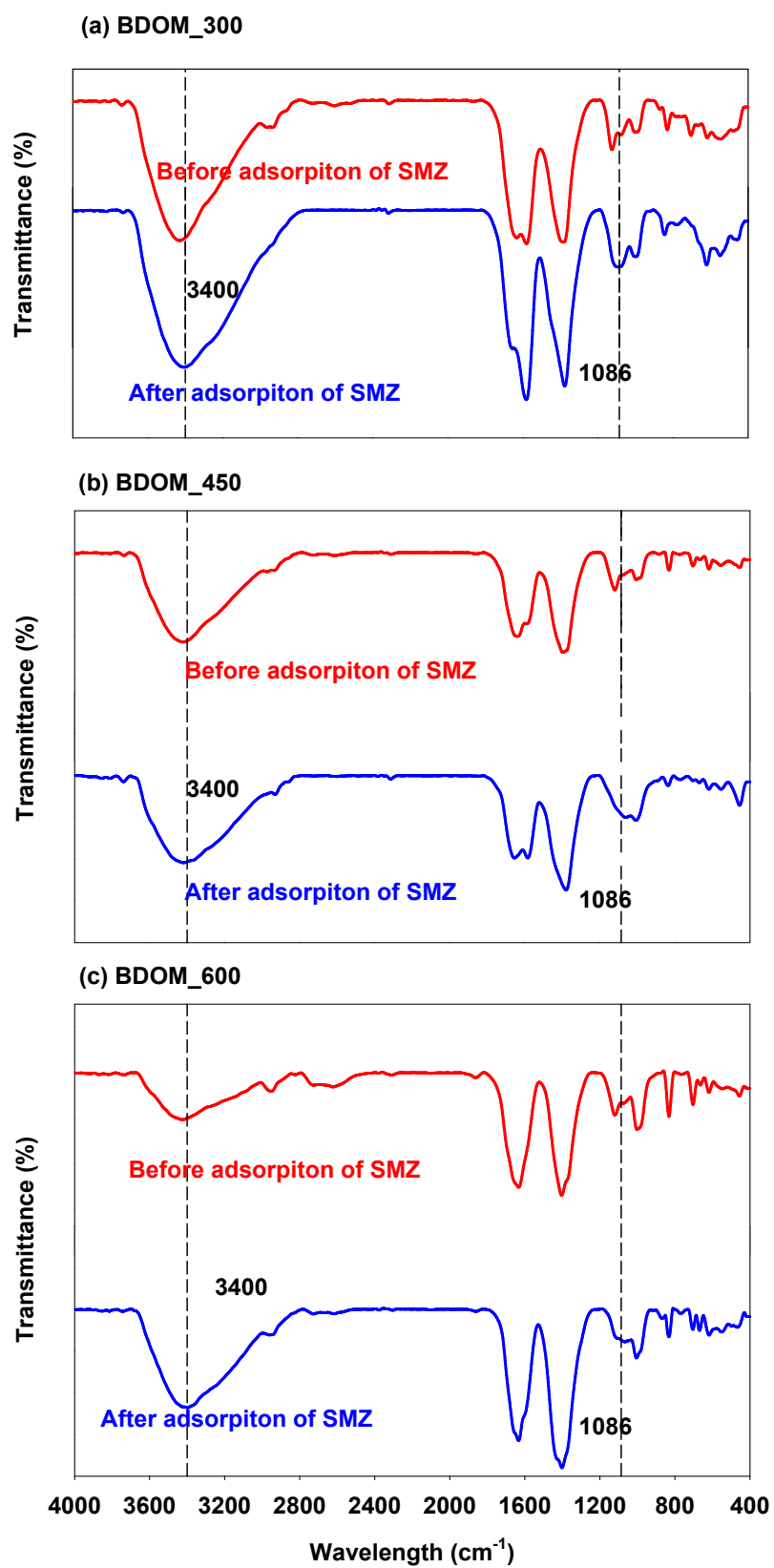


Fig. S5. Fourier transform infrared (FTIR) spectra of BDOMs before and after SMZ adsorption.

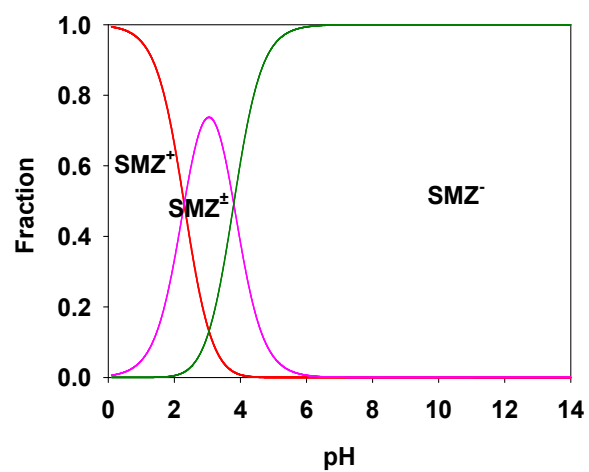


Fig. S6. pH-dependent speciation of the whole SMZ molecular and the functional groups, respectively.

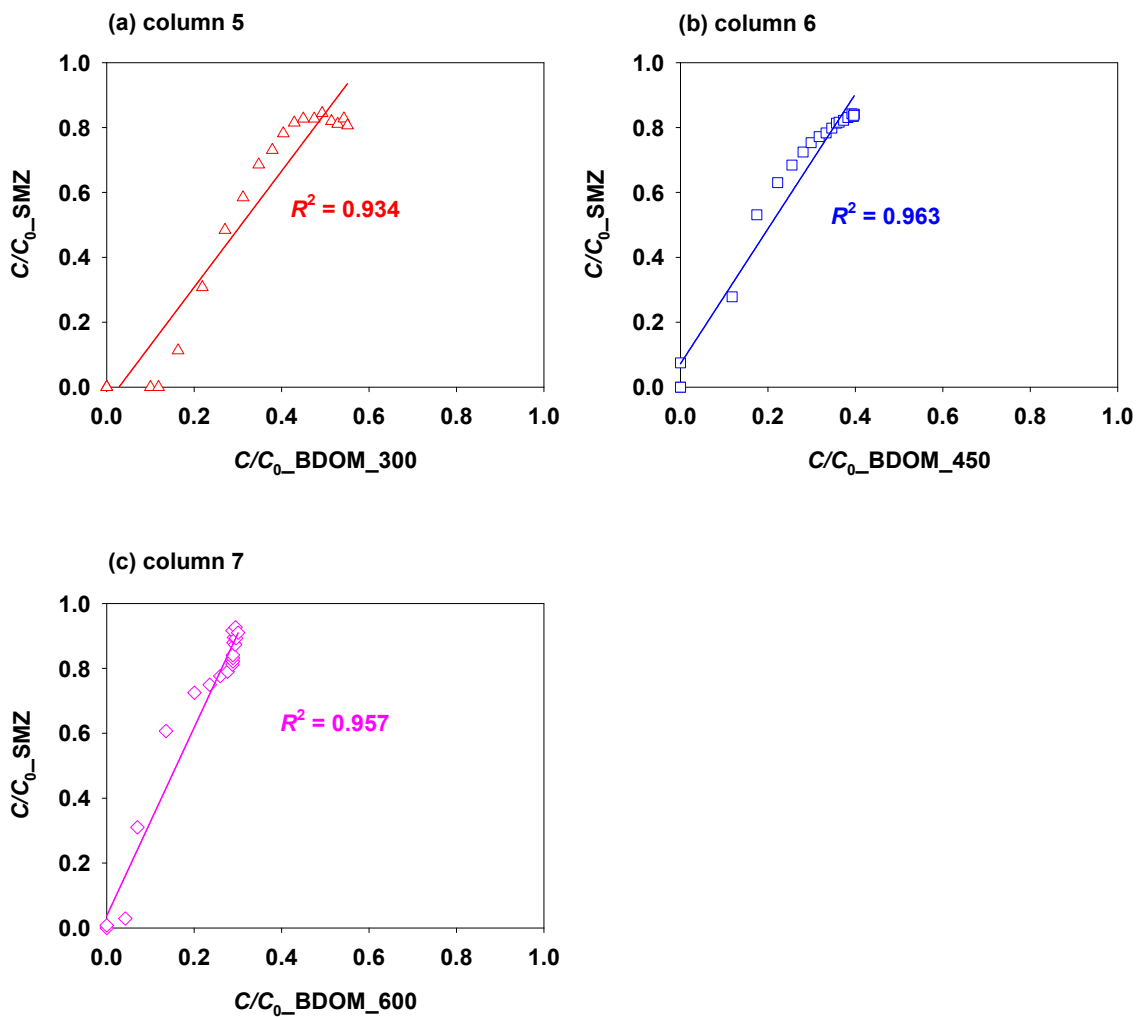


Fig. S7. Comparison of montmorillonite colloids breakthrough and CIP breakthrough after 0.8 PV in the respective effluent for columns 5–7.

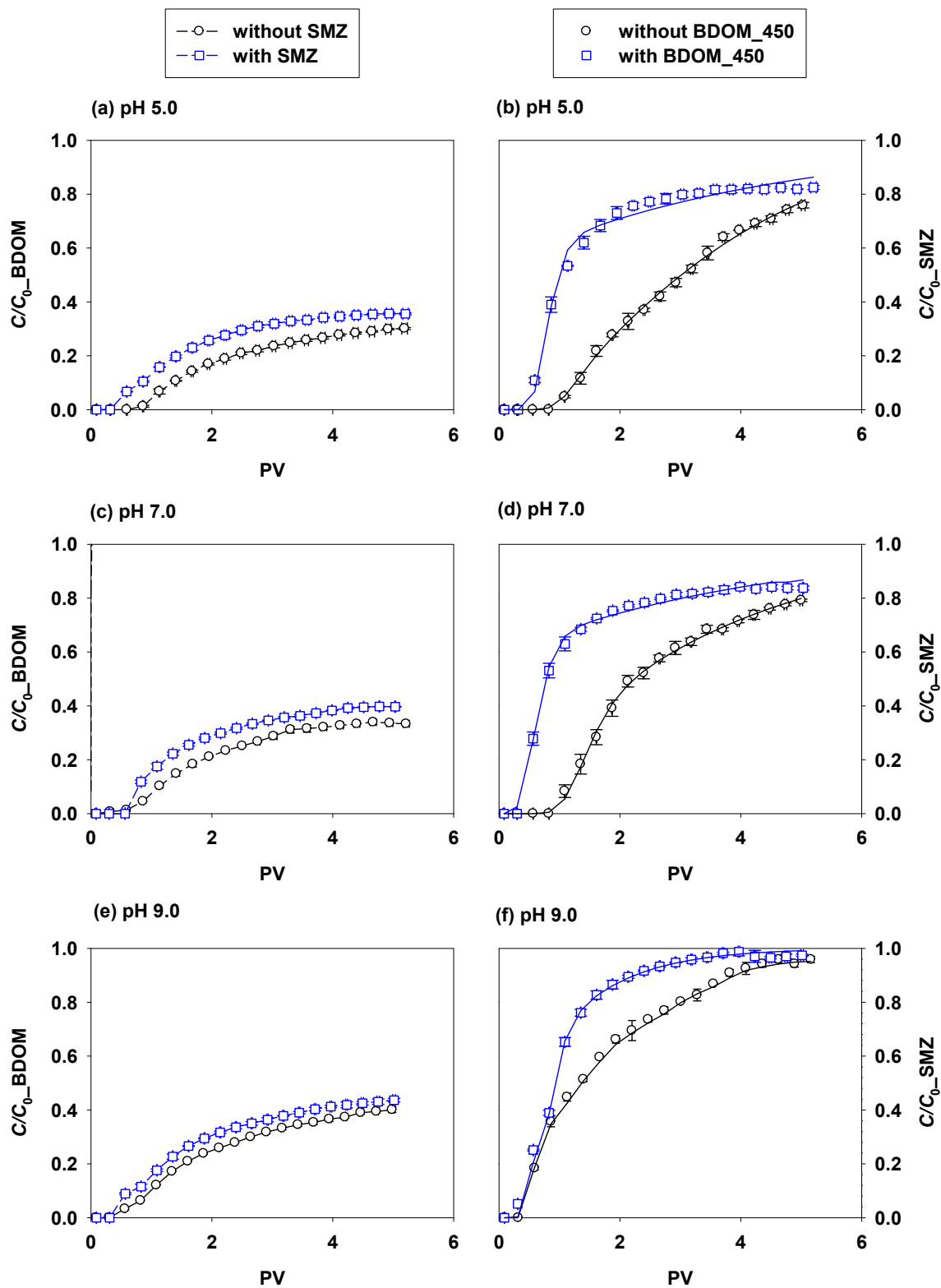


Fig. S8. Co-transport of BDOM_450 and SMZ in saturated soil columns at different pH conditions (the ionic strength was 10 mM NaCl): (a) and (b) Breakthrough curves of BDOM and SMZ at pH 5.0 (columns 2, 4, and 6, Table S4), respectively; (c) and (d) breakthrough curves of BDOM and SMZ at pH 7.0 (columns 8–10, Table S4),

respectively; and (e) and (f) breakthrough curves of BDOM and SMZ at pH 9.0 (columns 11–13, Table S4), respectively. Solid lines in the right plots are plotted by curve-fitting experimental data with the two-site non-equilibrium transport model.

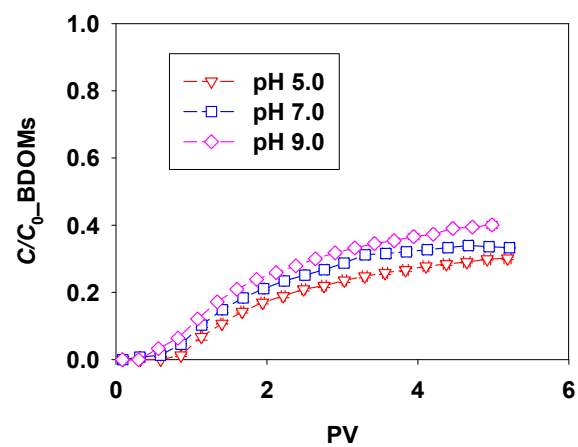


Fig. S9. Transport of BDOMs in soil under different pH conditions (at 10 mM NaCl).

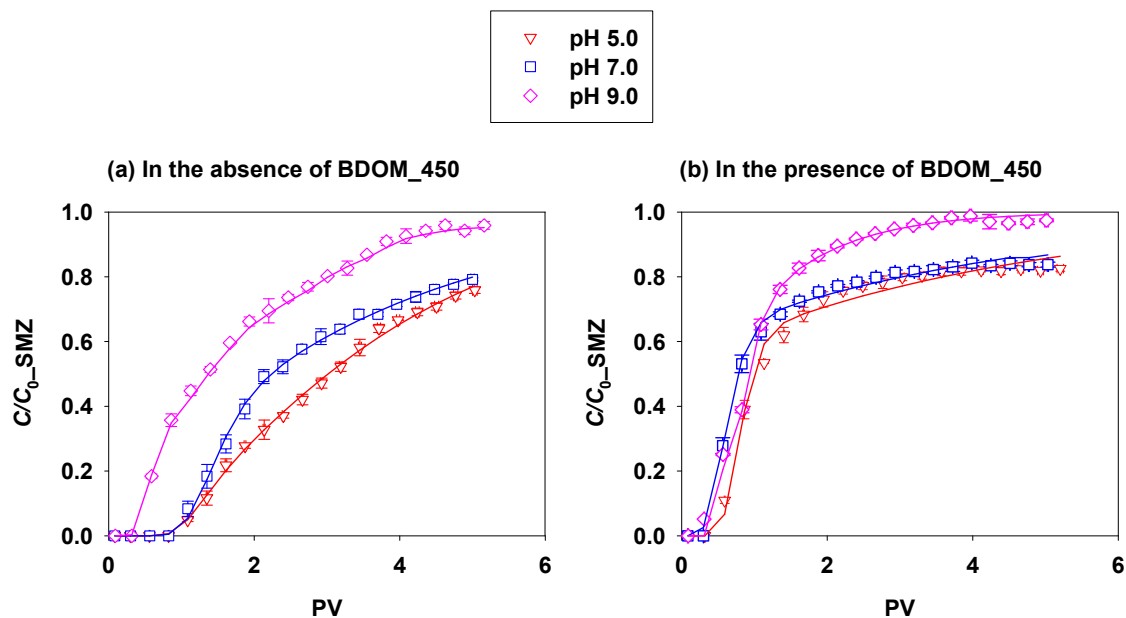


Fig. S10. Transport of SMZ in soil under different pH conditions (at 10 mM NaCl): (a) in the absence of BDOM and (b) in the presence of BDOM. Solid lines in the plots are plotted by curve-fitting experimental data with the two-site non-equilibrium transport model.

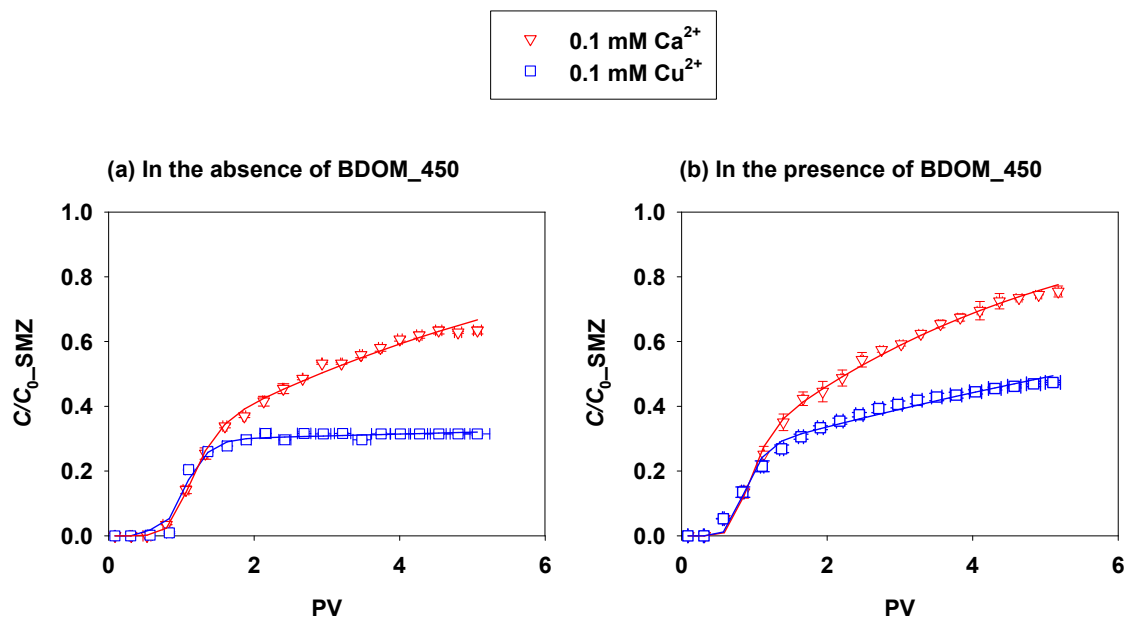


Fig. S11. Comparative transport of SMZ in soil in the presence of 0.1 mM Ca²⁺ and Cu²⁺ (at pH 5.0): (a) in the absence of BDOM_450 and (b) in the presence of BDOM_450. Solid lines in the plots are plotted by curve-fitting experimental data with the two-site non-equilibrium transport model.

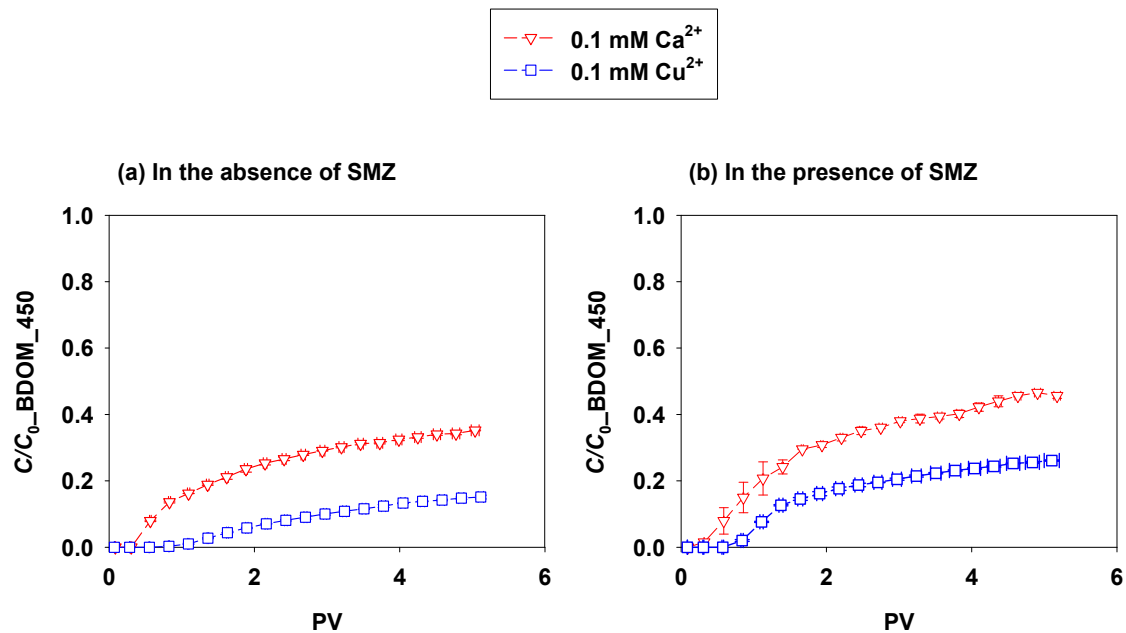


Fig. S12. Comparative transport of BDOM₄₅₀ in soil in the presence of 0.1 mM Ca^{2+} and Cu^{2+} (at pH 5.0): (a) in the absence of SMZ and (b) in the presence of SMZ.

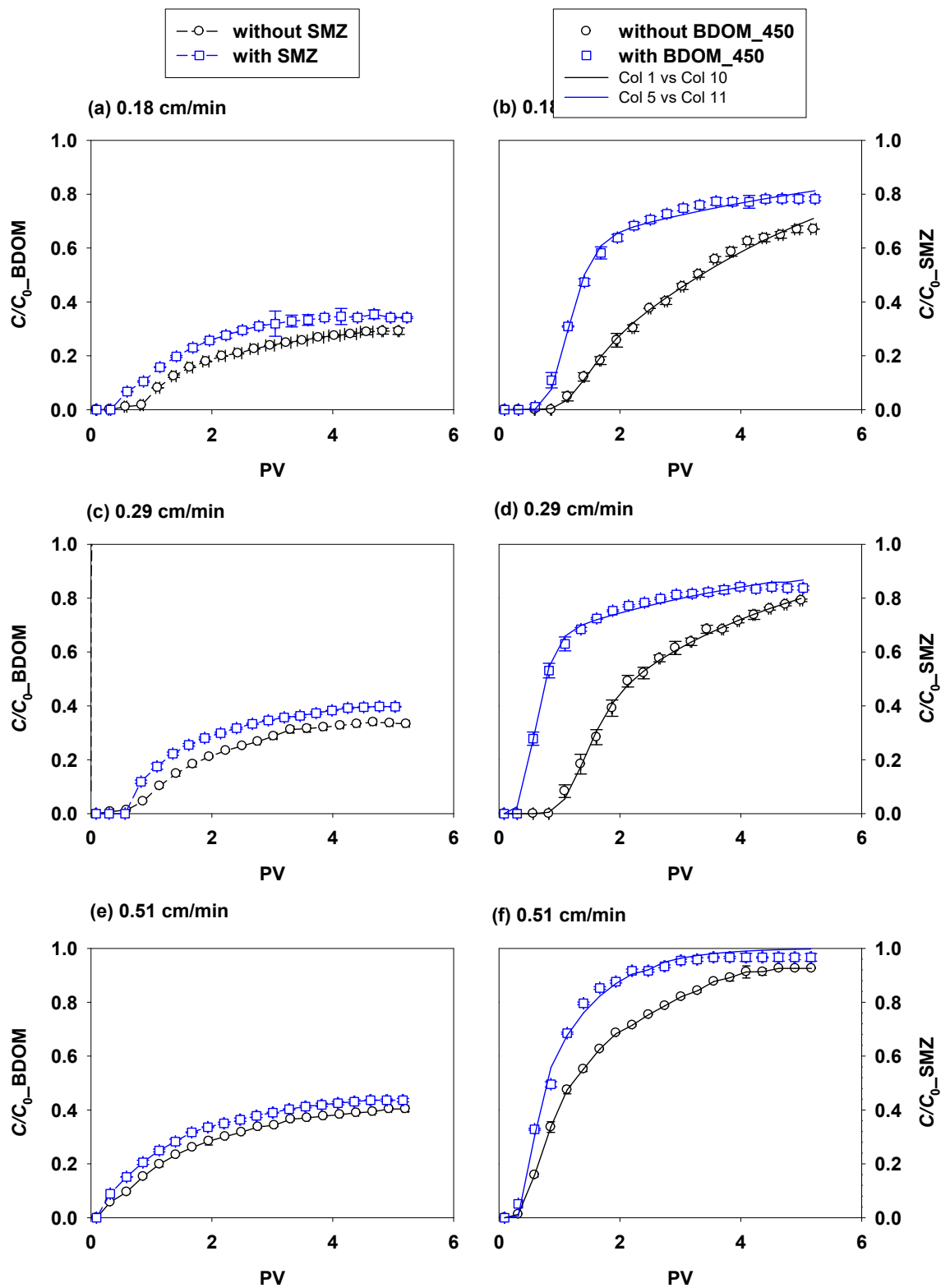


Fig. S13. Co-transport of BDOM_450 and SMZ in saturated soil columns under different flow rate conditions (10 mM NaCl, pH 7.0): (a) and (b) Breakthrough curves of BDOM and SMZ at the flow rate of 0.18 cm/min (columns 20–22, Table S4), respectively; (c) and (d) breakthrough curves of BDOM and SMZ at the flow rate of 0.29 cm/min

(columns 2, 4, and 6, Table S4), respectively; and (e) and (f) breakthrough curves of BDOM and SMZ at the flow rate of 0.51 cm/min (columns 23–25, Table S4), respectively. Solid lines in the right plots are plotted by curve-fitting experimental data with the two-site non-equilibrium transport model.

References

- S1. G.W. Gee and D. Or, Particle size analysis. In Dane J, Topp C (eds.) *Methods of Sand Analysis*, *Sand Sci. Soc. Am. Madison.*, 2002, pp. 255–293.
- S2. M. Abdelwaheb, K. Jebali, H. Dhaouadi and S. Dridi-Dhaouadi, Adsorption of nitrate, phosphate, nickel and lead on soils: risk of groundwater contamination, *Ecotox. Environ. Safe.*, 2019, **179**, 182–187.
- S3. I. Chowdhury, N. D. Mansukhani, L. M. Guiney, M. C. Hersam and D. Bouchard, 2015. Aggregation and stability of reduced graphene oxide: Complex roles of divalent cations, pH, and natural organic matter. *Environ. Sci. Technol.*, 2015, **49**, 10886–10893.
- S4. J. R. Helms, A. Stubbins, J. D. Ritchie, E. C. Minor, D. J. Kieber and K. Mopper, Absorption spectral slopes and slope ratios as indicators of molecular weight, source, and photobleaching of chromophoric dissolved organic matter, *Limnol. Oceanogr.*, 2008, **53**, 955–969.
- S5. S. L. Walker, J. E. Hill, J. A. Redman and M. Elimelech, Influence of growth phase on adhesion kinetics of *Escherichia coli* D21g. *Appl. Environ. Microb.*, 2005, **71**, 3093–3099.
- S6. T. Xia, P. Ma, Y. Qi, L. Zhu, Z. Qi and W. Chen, Transport and retention of reduced graphene oxide materials in saturated porous media: synergistic effects of enhanced attachment and particle aggregation. *Environmental pollution Environ. Pollut.*, 2019, **247**, 383–391.
- S7. K. Sun, S. Dong, Y. Sun, B. Gao, W. Du, H. Xu and J. Wu, Graphene oxide-facilitated transport of levofloxacin and ciprofloxacin in saturated and unsaturated porous media, *J. Hazard. Mater.*, 2018, **348**, 92–99.

- S8. Y. Xing, X., Chen, X., Chen, J., Zhuang, Colloid-mediated transport of pharmaceutical and personal care products through porous media. *Sci. Rep.*, 2016, **6**, 35407.
- S9. F. Wang, J. J. H. Haftka, T. L. Sinnige, J. L. M. Hermens and W. Chen, Adsorption of polar, nonpolar, and substituted aromatics to colloidal graphene oxide nanoparticles. *Environ. Pollut.*, 2014, **186**, 226–233.
- S10. N. Toride, F.J. Leij and M.T. van Genuchten, *The CXTFIT code for estimating transport parameters from laboratory or field tracer experiments*, Res. Report, 1999.
- S11. P.R. Kasten, L. Lapidus and N.R. Amundson, Mathematics of adsorption in beds. V. effect of intra-particle diffusion in flow systems in fixed beds, *J. Phys. Chem.*, 1952, 56 (6), 683–688.
- S12. P. Nkedi-Kizza, J.W. Biggar, H.M. Selim, M.T. Van Genuchten, P.J. Wierenga and J.M. Davidson, On the equivalence of two conceptual models for describing ion exchange during transport through an aggregated oxisol, *Water Res. Res.*, 1984, 20, 1123–1130.
- S13. M.T. van Genuchten and R.J. Wagenet, Two-site/two-region models for pesticide transport and degradation: theoretical development and analytical solutions, *Soil Sci. Soc. Am. J.*, 1989, 53, 1303–1310.
- S14. R. Wikiniyadhanee, S. Chotpantarat and S.K. Ong, Effects of kaolinite colloids on Cd^{2+} transport through saturated sand under varying ionic strength conditions: column experiments and modeling approaches, *J. Contam. Hydrol.*, 2015, 182, 146–156.
- S15. D. Kuntz, and P. Grathwohl, Comparison of steady-state and transient flow conditions on reactive transport of contaminants in the vadose soil zone, *J. Hydrol.*, 2009, 369, 225–233.

- S16. H. Chen, B. Gao, H. Li and L. Q. Ma, Effects of pH and ionic strength on sulfamethoxazole and ciprofloxacin transport in saturated porous media, *J. Contam. Hydrol*, 2011, 126, 29–36.
- S17. M. B. Ahmed, J. H. Zhou, H. H. Ngo, W., Guo, M. A. H. Johir and K. Sornalingam, Single and competitive sorption properties and mechanism of functionalized biochar for removing sulfonamide antibiotics from water. *Chem. Eng. J.*, 2017, **311**, 348–358.
- S18. M. Teixido, J.J. Pignatello, J.L. Beltran, M. Granados, J. Peccia, Speciation of the ionizable antibiotic sulfamethazine on black carbon (biochar), *Environ. Sci. Technol.*, 2011, **45**, 10020–10027.
- S19. W. Chen, R. Wei, L. Yang, Y. Yang, G. Li and J. Ni, Characteristics of wood-derived biochars produced at different temperatures before and after deashing: Their different potential advantages in environmental applications. *Sci. Total Environ.*, 2019, **651**, 2762–2771.
- S20. M. Keiluweit, P.S. Nico, M.G. Johnson, M. Kleber, Dynamic molecular structure of plant biomass-derived black carbon (biochar). *Environ. Sci. Technol.*, 2010, **44**, 1247–1253.